Regular Article

PHYSICAL CHEMISTRY RESEARCH
Published by the
Iranian Chemical Society
www.physchemres.org
info@physchemres.org

***Phys. Chem. Res.**, Vol. 3, No. 2, 89-98, June 2015.*
DOI: 10.22036/pcr.2015.7790

Size Evolution Study of the Electronic and Magnetic Properties of MgO Nanoclusters

A. Mohajeri* and A. Omidvar
Department of Chemistry, College of Sciences, Shiraz University, Shiraz, Iran
(Received 14 November 2014, Accepted 16 January 2015)

Magnesium oxide nanoclusters have attracted much attention due to their potential applications to catalysis and novel optoelectronic materials. In the present study, we have studied the electronic and magnetic properties of the stoichiometric magnesium oxide nanoclusters $(MgO)_n$ for n = 2-20. Although the binding energy increases with the size of the cluster, it reaches the asymptotic limit of about 66.0 eV per unit for relatively large n value. The static dipole polarizability also exhibits distinct size dependence, reflecting clearly the structural transition when the cluster grows. The polarizability and the binding energy of the clusters are found to be inversely related to each other and their correlation is rationalized by invoking the minimum polarizability principle. Moreover, principle of maximum hardness is also used to characterize the magic number clusters. A well-defined linear correlation is found between static dipole polarizability and the inverse of ionization potential. The most important feature of this work is the NMR study of MgO clusters which is reported for the first time. For each cluster size, the calculated NMR parameters at ^{17}O nuclei together with electronic and structural data provide detailed insight into the properties of bulk and in particular of nanosized structures. Variation of ^{17}O chemical shieldings demonstrates the electrostatic environment divisions around the oxygen nuclei which in turn originate from the cluster structure and its symmetry.

Keywords: MgO nanoclusters, Chemical shielding, NMR, MPP, PMH

INTRODUCTION

Clusters are of great experimental and theoretical interest, because they may be considered to form the bridge between the microscopic (atoms, molecules) and the macroscopic forms of matter. In this context, problems related to the qualitative differences between clusters of various sizes and bulk as well as the dependence of the properties of clusters on their size, are of great scientific and technological interest. In experiments, mass spectra are used to reveal the stability of different cluster sizes and infrared spectra could give characteristic information about structures of the cluster. Meanwhile, theoretical calculations are necessary to study the evolution of structure and properties with the cluster size.

Amongst different metal-oxide nanostructures, $(MgO)_n$ has emerged as a nanoscaled cluster of great interest. Magnesium oxide (MgO) is a prototype of simple metal oxides, which is widely used in technological applications. Its powder is considered as a kind of dopants to form high-temperature superconductor thick films [1,2] and also a very important metal oxide supporter of catalysis [3,4]. Bulk MgO is known as an inert material with a high melting point, as well as a typical wide gap insulator with band gap of 7.8 eV [5,6]. MgO nanomaterials such as nanorods [7], nanowires [8], nanotubes [9] and nanoflowers [10] have been synthesized. However, MgO clusters have received extensive attention both experimentally [11-13] and theoretically [14-21] in the past two decades.

Saunders carried out experiments in a triple quadrupole mass spectrometer for MgO clusters and observed mass spectrum which indicated the stability of $(MgO)_3$ subunits [22,23]. Ziemann and Castleman performed experimental measurements using laser-ionization time-of-flight mass

*Corresponding author. E-mail: amohajeri@shirazu.ac.ir

spectrometry and found ''magic clusters'' for $(MgO)_n$ clusters at n = 4, 6, 9, 12 and 15 [24].

Recently, small neutral gas phase $(MgO)_n$ clusters up to n = 16 were studied using a tunable IR-UV two-color ionization scheme to measure the vibrational spectra. This group also used density functional theory (DFT) to optimize the geometries generated by a hybrid genetic algorithm to find the global minimum and to predict the vibrational frequencies for $(MgO)_n$, n = 3-16 [25]. In addition, they also explored the structures of cationic MgO clusters [26]. The most recent treatment of $(MgO)_n$ clusters has been reported by Chen *et al.* [27] where they used tree growth-hybrid genetic algorithm to predict the global minima for $(MgO)_n$ nanoclusters. New lowest energy isomers were found for a number of $(MgO)_n$ clusters. Moreover, Neogi and Chaudhury [28] reported the growth as well as some properties of $(MgO)_n$ such as infrared spectra, vertical excitation energies.

Despite the aforementioned extensive studies, published experiences concerning the correlation between the stability and the electronic or magnetic properties of MgO clusters are still scare. One of the most important properties of the clusters is the static dipole polarizability which is due to its role in many significant phenomena and processes (*eg.*, light scattering and interaction phenomena) and technological applications (*eg.*, electronic devices). Accordingly, in this research we have extended our previous study on the static dipole polarizability and electronic properties of ZnS [29], ZnSe [30] and Al clusters [31] to MgO nanoclusters. In fact, we focus on the static dipole polarizability, stability function, and chemical hardness for the $(MgO)_n$ with n = 2-20. The size dependence of these reactivity descriptors and their relation to the relative stability of the clusters are discussed.

On the other hand, a wide variety of information including structural and conformational determination can be derived from the magnetic properties of certain nuclei such as oxygen. In this context, high sensitivity of nuclear magnetic resonance (NMR) signals to the electronic density at the sites of magnetic nuclei approves NMR as a prevailing tool for studying the structural features of various materials. Nonetheless, owing to the complexity in nanoclusters, direct exploring the electrostatic environments around the nuclei by practical spectrometry data is difficult. In this context, theoretical calculations can be better alternatives. Accordingly, we have also investigated the magnetic properties of MgO clusters by calculating the chemical shielding (CS) parameters at the ^{17}O nuclei. To the best of our knowledge, no NMR study of MgO clusters has been theoretically conducted thus far. However, CS parameters are useful to fully understand the local environment of atoms within the considered nanoclusters.

COMPUTATIONAL DETAILS

It is known that the potential energy surfaces of heteroatomic clusters are rich of stable local minima very close in energy [32]. In such kind of potential energy surfaces, the determination of the ground state is not an easy task. In this work we do not deal with searching the possible structures to find global minimum for each cluster, indeed we focus on the known lowest-energy structures which have been recently reported for neutral MgO clusters and investigate how the cluster properties change with size. Very recently, Chen *et al*. used the tree growth-hybrid genetic algorithm in conjunction with semiempirical molecular orbital calculations followed by B3LYP geometry optimizations to predict the global minima for $(MgO)_n$ nanoclusters [27]. To avoid trapping in the local minima of the potential energy surface, the lowest energy isomers of MgO clusters (n =2-20) reported in reference [27] were adopted in the present study. We have relied on the B3LYP method for re-optimization and calculation of the electronic and magnetic properties of the clusters under scrutiny. This method has been proven to be reliable for the geometric, stabilities and electronic properties of clusters [33,34]. We used DZVP basis set [35] for both magnesium and oxygen atoms. Frequency calculations have been carried out for all clusters at the same level of theory and the minimum energies were confirmed by the real frequencies. It should be mentioned that all considered clusters are closed shell systems with a singlet ground state.

The considered method and basis set have been also used to calculate NMR parameters based on the gauge independent atomic orbital (GIAO) approach [36]. The calculated CS tensors in principal axes system (PAS) ($\sigma_{33} > \sigma_{22} > \sigma_{11}$) are converted to measurable NMR parameters, CS isotropy (CS^I) and CS anisotropy (CS^A), by the use of

following equations

$$CS^I = (\sigma_{33} + \sigma_{22} + \sigma_{11})/3 \quad (1)$$

$$CS^A = \sigma_{33} - (\sigma_{22} + \sigma_{11})/2 \quad (2)$$

Moreover, the polarizabilty is the response of a molecule perturbed by an external field. When a molecule is set in a uniform electric field (**F**), the energy of the perturbed system (E(**F**)) may be expressed as power series of the electric field. The expansion coefficients allow the computations of the dipole moments, linear, and non linear polarizabilities. The static dipole polarizability is then

$$\alpha_{ij} = \frac{\partial \mu_i(\mathbf{F})}{\partial \mathbf{F}_j} = -\frac{\partial^2 \mathrm{E}(\mathbf{F})}{\partial \mathbf{F}_i \partial \mathbf{F}_j} \qquad i,j = x,y,z \quad (3)$$

Since the measured polarizability is the average $<\alpha> = 1/3\ tr(\alpha_{ij}) = (\alpha_{xx} + \alpha_{yy} + \alpha_{zz})/3$, it is sufficient to calculate only the diagonal components α_{ii} of the polarizability tensor. In this study, the magnitude of the infinitesimal field $\delta\mathbf{F}$ was chosen to be 10^{-3} a.u. The evolution of atomic charges has been also studied by employing natural population analysis (NPA). All calculations were carried out with the GAUSSIAN 09 suite of programs [37].

RESULTS AND DISCUSSION

The lowest energy structures for the $(MgO)_n$ clusters (n = 2-20) are presented in Fig. 1. As mentioned before, details of the structural analysis of the clusters have been studied in a recent paper [27] and thus will not be discussed in the present work. However, the obtained structures provide an opportunity to explore different properties of clusters as well as their size evolution.

Our discussed properties in this work start with magnetic parameters followed by energetics and electronic descriptors.

Table 1 contains the chemical shielding of the ^{17}O nuclei for each of the studied clusters. In general, the CS^I parameter shows the average electronic density at the atomic site. Thus, differences in the reported CS^I (Table 1) are associated with the changes in the electrostatic environment around the oxygen nuclei originating from the

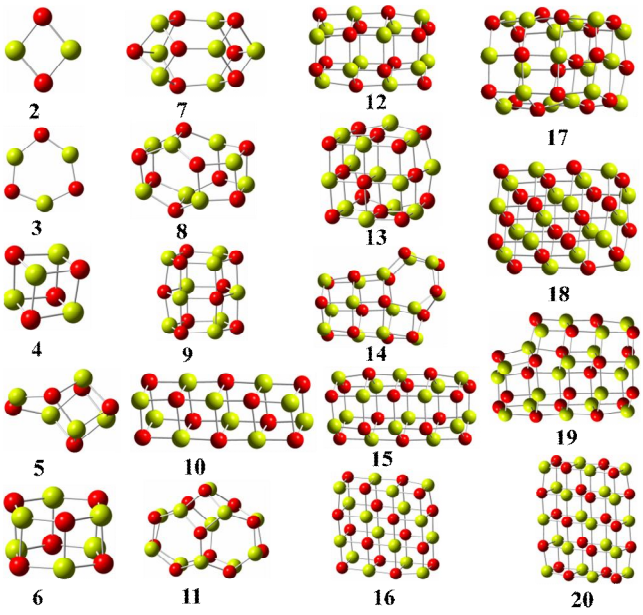

Fig. 1. Geometrical structures for the low energy $(MgO)_n$ calculated at B3LYP/DZVP level (n = 2-20).

cluster structure and its symmetry. Number of magnetically equivalent oxygens (shown in parenthesis) depends on the symmetry of the cluster. For instance, in the smaller sizes with n = 2-4 and 6, all oxygen nuclei are magnetically equivalent and thus one CS^I has been reported for each cluster. For larger clusters, the CS^I values are distributed in a wider range which are divided ino few groups. The groups have equivalent calculated CS^I and CS^A parameters which means that the nuclei in each group have equivalent electrostatic properties around similar nuclei. In order to calrify this division, we present atomic grouping for n = 5, 10, 15 and 20 as representative examples in Fig. 2. As the figure shows for n = 5, 10, 15 and 20 the oxygens are, respectively, classified into 4, 3,3, and 4 groups. For instance, in $(MgO)_{10}$ three distinct values of CS^I indicate that 10 oxygens are divided into 3 groups in which different electrostatic environments are experienced. In the first group (G1), oxygens of the outer layers (O6, O10, O11, O15) have smaller CS^I of about 240 ppm. The CS^I increases by going to the inner layers and the maximum CS^I value (277 ppm) is observed for the oxygens of the middle layer

Table 1. ^{17}O Chemical Shielding Parameters (ppm) for $(MgO)_n$ Clusters with n = 2-20. The Numbers in the Parenthesis Indicate Number of Magnetically Equivalent Oxygens for Each CS^I Value

n	CS^I	CS^A
2	213 (2)	272.6
3	297 (3)	133.9
4	230 (4)	88.5-89.7
5	230 (1), 240 (2), 250 (1), 295 (1)	48.4-131.5
6	262.9 (6)	67.0-67.8
7	239 (1), 246 (3), 269 (2)	46.7-86.9
8	261 (4), 273 (4)	42.9-66.7
9	244 (3), 267 (6)	16.9-54.4
10	241 (4), 255 (4), 277 (2)	50.6-103.2
11	261 (2), 269 (2), 275 (5), 281 (2)	16.7-56.6
12	252 (6), 264 (6)	21.5-58.1
13	222 (4), 241 (5), 255 (4)	16.7-89.7
14	248- 253 (4), 257-260 (3), 263 (5), 270-273 (2)	16.8-72.2
15	249-251 (6), 257-258 (3), 262 (6)	15.5-55.7
16	243 (4), 248 (4), 252 (8)	16.1-103.7
17	244 (4), 249 (4), 255 (5), 275 (4)	2.2-39.5
18	241 (1), 243 (4), 245 (4), 246 (4), 247 (1) 253 (4)	2.2-39.5
19	235 (1), 245-250 (10), 255-265 (7), 267 (1)	16.5-99.0
20	242 (4), 246-248 (10), 251 (4), 262 (2)	9.5-104.5

(O8, O13). On the other hand, the CS^A parameter indicates the difference between the distribution of the electronic densities perpendicular to the molecular plane and within the molecular plane. Thus, large CS^A values for the planar structure ($(MgO)_2$ and $(MgO)_3$) indicate that the distribution of electronic density at the oxygen in the perpendicular plane is greater than that of the molecular plane. This observation can be attributed to the electronic density mainly localized in the p-orbitals as a lone pair. On the contrary, for larger clusters the oxygens have been connected to four Mg atoms leading to reduction of the perpendicular electron localization and results in smaller CS^A values.

Now, we turn our attention to the electronic properties of the considered clusters collected in Table 2. The calculated dipole moments indicate that most of the studied clusters have relatively small dipole moments, reflecting the roughly inverse symmetric distribution of electron density within these clusters. Indeed, the higher symmetry often leads to a relatively low dipole moment for different structures. Although the Mg-O bond is very polarized, the local dipole moments are mostly cancelled by the alternative arrangement of Mg and O atom. Therefore, most of the stable structures possess small dipole moments. Several large dipole moments are found in the low-lying structures with odd number of MgO units, specifically, n = 5, 7, 13 and 17 in which their asymmetric electron density distribution leads to the relatively large dipole moments.

As a stability criterion, we have computed binding energy per MgO unit

$$\mathrm{BE}(n) = \frac{n\,\mathrm{E(Mg)} + n\,\mathrm{E(O)} - \mathrm{E(MgO)}_n}{n} \qquad (4)$$

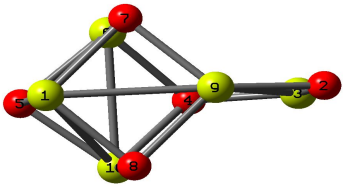

G1: O5 CS^I =230
G2: O7,O8 CS^I = 240
G3: O4 CS^I = 250
G4: O2 CS^I =295

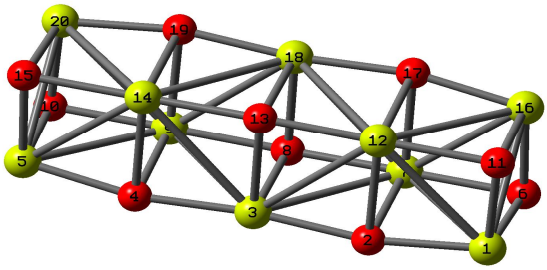

G1: O6,O10,O11,O15 CS^I =240
G2: O2,O4,O17,O19 CS^I = 255
G3: O8,O13 CS^I = 277

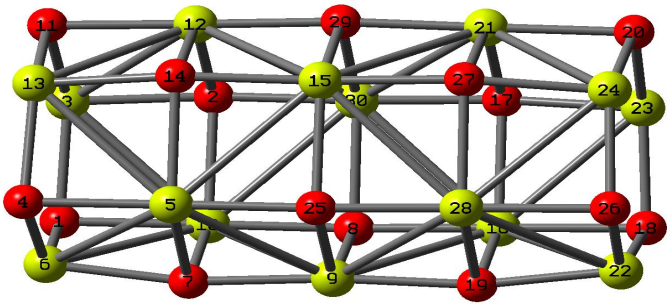

G1: O2,O7,O14,O17,O19,O27 CS^I =249-251
G2: O8,O25,O29 CS^I = 257-258
G3: O1,O4,O6,O11,O18,O28 CS^I = 262

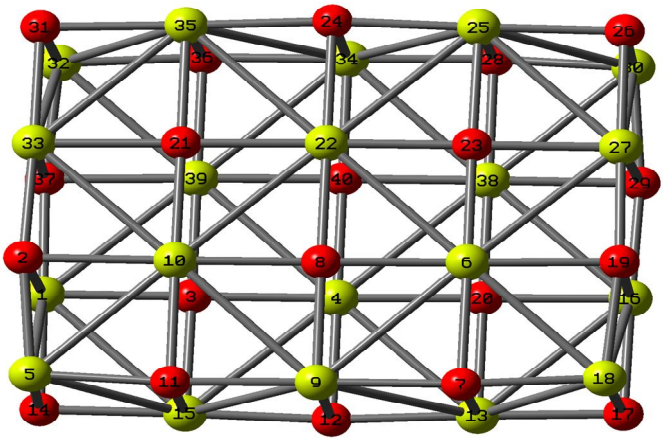

G1: O14,O17,O26,O31 CS^I =242
G2: O3,O7,O8,O11,O20,O21, O23,O28,O36,O40 CS^I = 246-258
G3: O2,O19,O29,O37 CS^I = 251
G4: O12,O24 CS^I =260

Fig. 2. CS^I grouping for $(MgO)_n$ with n = 5,10,15, and 20 as representative examples.

Table 2. Calculations of Dipole Moment (μ), the Binding Energy (BE), Stability Function (SF), Mean Static Polarizability (<α>), Differential Mean Polarizability per Unit (δα), Chemical Hardness (η), and the Range of Natural Atomic Charges on Oxygen Atoms (q_O) for the Lowest Energy Structures of $(MgO)_n$ Clusters (n = 2-20)

n	μ (Debye)	BE (n) (eV)	SF(n) (eV)	< α> (Å^3)	δα (Å^3)	η (eV)	q_O (e)
2	0.00	62.688	-0.544	7.770	-2.876	1.36	-1.449
3	0.03	63.867	0.000	9.664	-3.539	2.07	-1.527
4	0.00	64.457	1.088	11.517	-3.881	1.95	-1.493
5	3.64	64.593	-2.721	14.850	-3.791	1.69	-1.462 - -1.531
6	0.05	65.137	2.721	16.146	-4.070	2.23	-1.510
7	1.51	65.137	-1.905	19.038	-4.041	2.03	-1.494 - -1.516
8	0.07	65.375	-0.272	21.218	-4.108	2.20	-1.506 - -1519
9	0.09	65.591	2.177	23.118	-4.192	2.32	-1.495 - -1.507
10	0.00	65.545	-1.633	26.170	-4.144	2.08	-1.479 - -1.493
11	0.51	65.657	-0.816	28.700	-4.151	2.24	-1.508 - -1.529
12	0.04	65.817	2.721	30.205	-4.243	2.37	-1.490 - -1.495
13	5.48	65.744	-1.633	32.880	-4.231	1.75	-1.459 - -1.481
14	0.38	65.798	-1.361	35.651	-4.214	2.23	-1.490 - -1.518
15	0.02	65.935	1.361	37.370	-4.269	2.42	-1.475 - -1.498
16	0.04	65.970	0.816	39.533	-4.290	4.29	-1.443 - -1.473
17	8.30	65.953	-1.905	42.218	-4.277	2.08	-1.419 - -1.499
18	0.02	66.044	2.177	43.906	-4.321	4.18	-1.406- -1.473
19	1.07	66.011	-2.177	47.034	-4.285	2.09	-1.460 - -1.496
20	0.03	66.089	-	48.868	-4.317	4.38	-1.427- -1.474

In Fig. 3 we show the binding energy variation for the energetically lowest isomers of $(MgO)_n$ with n up to 20. When considering large clusters, convergence towards an average binding energy around 66.0 eV per MgO unit can be recognized. Besides the overall stability of the clusters, the high stability of the so-called "magic-numbered" clusters has also become a subject of great interest. A cluster is considered particularly stable if its binding energy per unit is larger than that of the two neighboring clusters. This can be quantified through the stability function,

$$SF(n) = E(MgO)_{n+1} - E(MgO)_{n-1} - 2E(MgO)_n \quad (5)$$

This function, that has maxima for particularly stable clusters , is shown in Fig. 4. Here, we can identify particularly stable clusters for n = 4, 6, 9, 12, 15 and 18 implying that these clusters are more stable than their neighboring sizes. However, the most pronounced peaks occur at n = 6 and 12 indicating the maximum relative stability for $(MgO)_6$ and $(MgO)_{12}$. The high stability for these magic clusters is correlated with drastic changes in structure towards higher symmetry. For both clusters the hexagonal building blocks leads to more compact atomic arrangement and higher stability.

After the energetic analysis, the static dipole polarizability of the considered clusters has been explained to trace the effect of size and dimensionality on this property. In fact, the static dipole polarizability is a fundamental property of a molecule which governs a variety of physical and chemical phenomena. It expresses the

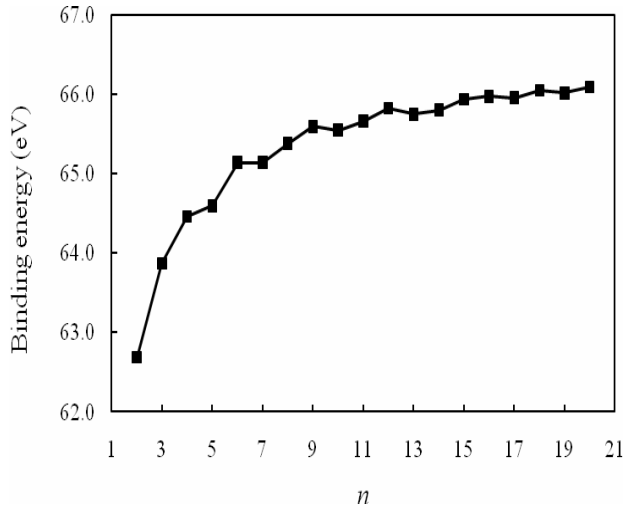

Fig. 3. Variation of binding energy with size for $(MgO)_n$ clusters (n = 2-20).

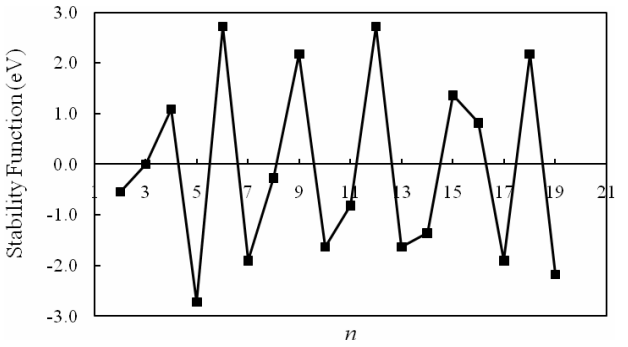

Fig. 4. Variation of stability function with size for $(MgO)_n$ clusters (n = 2-20).

induced dipole moment value of the molecule under the effect of a weak external field. Thus, it can be taken as a measure of the stability of the electronic distribution. The minimum polarizability principle (MPP) was indeed formulated, which states that "the natural evolution of any system is toward a state of minimum polarizability" [38]. This implies $\langle\alpha_M\rangle < \sum_i \langle\alpha_i\rangle$ where $\langle\alpha_M\rangle$ is the cluster mean dipole polarizability and $\langle\alpha_i\rangle$ is the mean polarizability of the constituent fragments. However, the MPP does not always hold [39] and the reasons are not fully understood. The MPP is conceptually related to principle of maximum hardness (PMH) based on the absolute hardness definition [40]

$$\eta = \frac{1}{2}\left(\frac{\partial^2 E}{\partial N^2}\right)_{\upsilon(r)} \cong \frac{1}{2}(IP - EA) \quad (6)$$

where N is the number of electrons and IP and EA are the ground state ionization potential and electron affinity, respectively. Chemical hardness has been established as an electronic quantity which may be used to characterize the relative stability of molecules. This quantity is associated with the concept PMH which states "molecules arrange themselves so as to be as hard as possible". Maximum hardness, minimum polarizability, and molecular stability complement each other. To study the correlation between the cluster stability with polarizability and hardness we have checked the applicability of MPP and PMH among the considered MgO clusters.

Here, we focus on the static dipole polarizability per MgO unit, which is calculated as $< \alpha(MgO)_n > / n$. The size evolution of the calculated mean polarizability has been shown in Fig. 5. As a natural extension of MPP, those clusters with the local minimum polarizability are more stable than the neighboring clusters. The observation of minimum at n = 4, 6,9,12, 15 and 18 is consistent with our discussion on the stability by energetic analysis for MgO clusters. Further, Fig. 6 clearly shows that the magic clusters are harder than their neighboring clusters, implying that both MPP and PMH can be hold as useful descriptors to determine the stability of MgO clusters.

In addition, a more sensitive quantity of interest is $\delta\alpha$,

$$\delta\alpha = \frac{< \alpha(MgO)_n >}{n} - < \alpha(MgO) > \quad (7)$$

This difference has been called by Maroulis *et al*. differential mean polarizability per unit and provides information for the delocalization of the electronic density in the cluster with respect to an equivalent number of non-interacting units [41]. Inspection in the reported $\delta\alpha$ in Table 2 reveals that the differential polarizability exhibits similar trend to mean polarizability. Moreover, the calculated $\delta\alpha$ are negative for all clusters indicating strong binding effect.

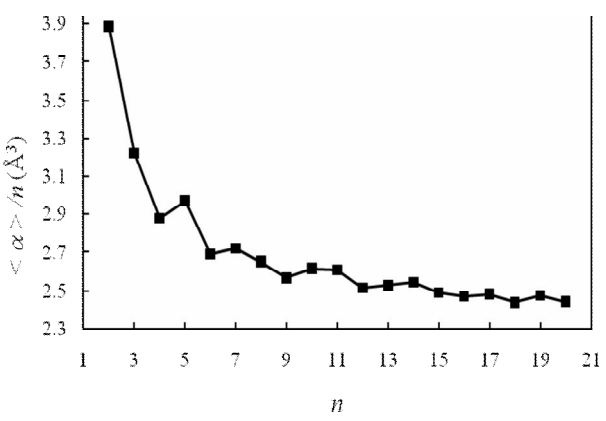

Fig. 5. Static polarizability per MgO unit of the lowest energy $(MgO)_n$ clusters as a function of the cluster size.

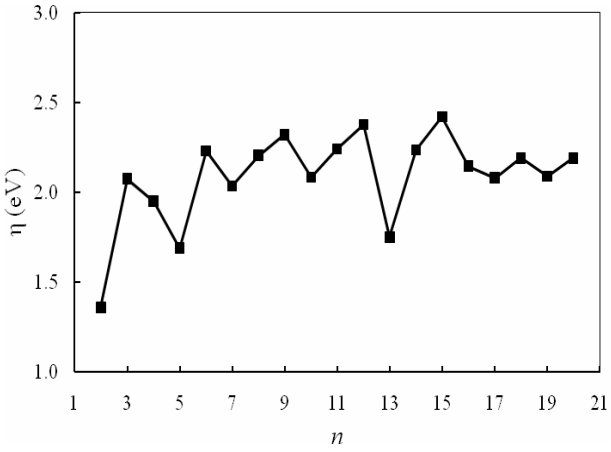

Fig. 6. Chemical hardness of the lowest energy $(MgO)_n$ clusters as a function of the cluster size.

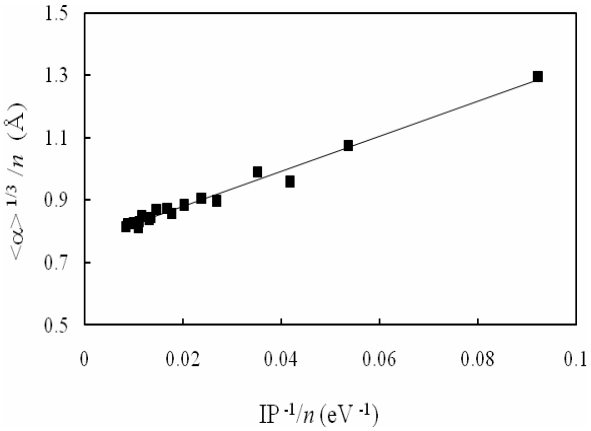

Fig. 7. The correlation between the cube root of mean polarizabilities per MgO unit and the inverse of the ionization potential for $(MgO)_n$ clusters.

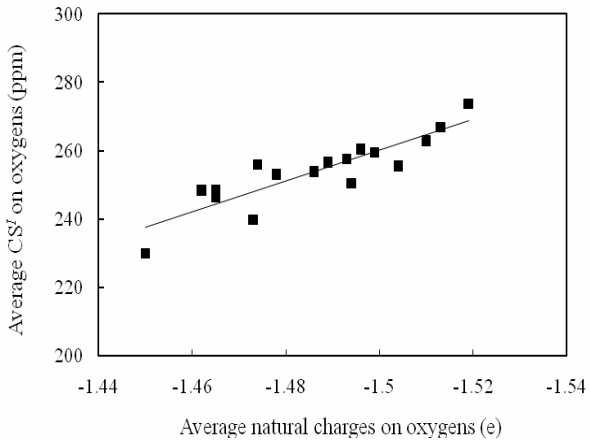

Fig. 8. Average of ^{17}O CS^I with respect to the average natural charge on oxygens for $(MgO)_n$ clusters (n = 4-20).

Also the results indicate that the more negative the calculated δα, the stronger the MgO units bind. Thus, both the mean and differential polarizability are connected with stability for MgO clusters.

It is known that the static dipole polarizability is a measure of the distortion of the electronic density and the information about the response of the system under the effect of an external static electric field. On the other hand, the ionization potential reveals how tightly an electron is bound within the nuclear attractive field of the systems. Dmitrieva and Plindov were the first to obtain a relationship between the polarizability and the ionization potential for atomic systems using a statistical model [42]. Recently, in our research group, the correlations between the cube root of polarizability and the inverse of the ionization potential have been confirmed for some molecular clusters [28,29]. Accordingly, in the present work, we have examined the existence of such correlation for the studied MgO clusters. Figure 7 displays that the cube root of mean polarizability per MgO unit increases linearly with increasing the inverse

of ionization potential per MgO unit. The corresponding linear correlation coefficient is found to be 0.983 indicating the reliability of the correlation. This is an important observation which can provide a way to calculate the polarizability of the larger size of clusters from the values of their ionization potential.

Finally, it is also of interest to have a look at the calculated atomic charges reported in the Table 2. As for other properties, the charge distribution in nanoclusters depends on their size. Inspection of the natural charge on oxygen atoms reveals that the electrostatic environment around the oxygen nuclei is an influential factor on the calculated natural charges. Apart from atom by atom analysis in each cluster, we also focused on the average charge on oxygen atoms in different size of MgO clusters. It is worth mentioning that we observed a correlation between the charge variation and chemical shielding for considered clusters. Figure 8 shows that excluding planar clusters (n = 2 and 3), for other considered structures (n = 4-20) the average ^{17}O CS^I is linearly correlated with the average natural charge on the oxygen atoms. Thus, in general, the overall shielding is larger for the clusters having more negative charge on oxygens.

CONCLUSIONS

The size dependence of electronic and magnetic properties such as relative stability, dipole moment, static dipole polarizability, chemical hardness, and chemical shielding have been studied for $(MgO)_n$ clusters (n = 2-20). Although the Mg-O bond is very polarized, most of the stable structures possess small dipole moments. In fact, the high symmetry of most studied structures leads to cancellation of the local dipole moments by alternative arrangement of Mg and O atom.

Energetic analysis shows that the $(MgO)_n$ clusters with $n = 3m$ and m = 2-6 are magic-size clusters and show enhanced stability. The static polarizability per unit decreases slowly with increasing cluster size, accompanied by some local oscillations. The MPP and PMH can be also used to characterize the stability of magic clusters. The maximum hardness, minimum polarizability, and cluster stability complement each other. It is found that the size-dependent polarizability and ionization potential of the MgO clusters strongly correlate with each other. These results will have some important implications in calculating the polarizability of these clusters in terms of the ionization potential directly. The most important feature of this work is the NMR study of MgO clusters which has been reported for the first time. In fact, the calculated NMR parameters together with electronic and structural data provide detailed insight to the nanosized clusters. In each cluster, n oxygen atoms were classified into few groups according to their CS^I values. The differences in CS^I associate with the changes in the electrostatic environment around the oxygen nuclei originating from the cluster structure and its symmetry. Furthermore, a linear correlation is found between the charge variation and chemical shielding of oxygen nuclei in considered clusters.

REFERENCE

[1] A. Bhargava, J.A. Alarco, I.D.R. Mackinnon, D. Page, A. Ilyushechkin, Mater. Lett. 34 (1998) 133.

[2] Y.S. Yuan, M.S. Wong, S.S. Wang, J. Mater. Res. 11 (1996) 8.

[3] S.H.C. Liang, I.D. Gay, J. Catal. 101 (1986) 293.

[4] H. Tsuji, F. Yagi, H. Hattori, H. Kita, J. Catal. 148 (1994) 759.

[5] S.H. Tamboli, R.B. Patil, S.V. Kamat, V. Puri, R.K. Puri, J. Alloys Compd. 477 (2009) 855.

[6] L. Hong , H. Wang, J. Cheng , L. Tang, J. Zhao, Comp. Theor. Chem. 980 (2012) 62.

[7] P.D. Yang, C.M. Lieber, Science 273 (1996) 1836.

[8] Y.D. Yin, G.T. Zhang, Y.N. Xia, Adv. Funct. Mater. 12 (2002) 293.

[9] J.H. Zhan, Y. Bando, J.Q. Hu, D. Golberg, Inorg. Chem. 43 (2004) 2462.

[10] X.S. Fang, C.H. Ye, L.D. Zhang, J.X. Zhang, J.W. Zhao, P. Yan, Small 1 (2005) 422.

[11] E. Puente, A. Aguado, A. Ayucla, J.M. Lo´pez, Phys. Rev. B 56 (1997) 7607.

[12] D. van Heijnsbergen, G. von Helden, G. Meijer, M.A. Duncan, J. Chem. Phys. 116 (2002) 2400.

[13] M. Gutowski, P. Skurski, X. Li, L.S. Wang, Phys. Rev. Lett. 85 (2000) 3145.

[14] J.M. Recio, R. Pandey, A. Ayuela, A.B. Kunz, J. Chem. Phys. 98 (1993) 4783.

[15] A. Jain, V. Kumar, M. Sluiter, Y. Kawazoe, Comput. Mater. Sci. 36 (2006) 171.
[16] J. Carrasco, F. Illas, S.T. Bromley, Phys. Rev. Lett. 99 (2007) 235502.
[17] R.B. Dong, X.S. Chen, X.F. Wang, W. Lu, J. Chem. Phys. 129 (2008) 044705.
[18] L. Chen, C. Xu, X.F. Zhang, C. Cheng, T. Zhou, Int. J. Quantum Chem. 109 (2009) 349.
[19] Y. Zhang, H.S. Chen, B.X. Liu, C.R. Zhang, X.F. Li, Y.C. Wang, J. Chem. Phys. 132 (2010) 194304.
[20] K.E. El-Kelany, M. Ferrabone, M. Rérat, P. Carbonni`ere, C.M. Zicovich-Wilson, R. Dovesi, Phys. Chem. Chem. Phys. 15 (2013) 13296.
[21] Y. Zhang, H.S. Chen, Y.H. Yin, Y. Song, J. Phys. B: At. Mol. Opt. Phys. 47 (2014) 025102.
[22] W.A. Saunders, Z. Phys. D: At. Mol. Clusters 12 (1989) 601.
[23] W.A. Saunders, Phys. Rev. B 37 (1988) 6583.
[24] P.J. Ziemann, A.W. Castleman, J. Chem. Phys. 94 (1991) 718.
[25] M. Haertelt, A. Fielicke, G. Meijer, K. Kwapien, M. Sierka, J. Sauer, Phys. Chem. Chem. Phys. 14 (2012) 2849.
[26] K. Kwapien, M. Sierka, J. Döbler, J. Sauer, M. Haertelt, A. Fielicke, G. Meijer, Chem. Int. Ed. 50 (2011) 1716.
[27] M. Chen, A.R. Felmy, D.A. Dixon, J. Phys. Chem. A 118 (2014) 3136.
[28] S. Ganguly Neogi, P. Chaudhury, Struct. Chem. 25 (2014) 1229.
[29] A. Mohajeri, M. Alipour, Int. J. Quantum Chem. 111 (2011) 3841.
[30] A. Mohajeri, M. Alipour, Int. J. Quantum Chem. 111 (2011) 3888.
[31] M. Alipour, A. Mohajeri, J. Phys. Chem. A 114 (2010) 12711.
[32] W. Tang, Q. Zhou, Phys. Rev. E 86 (2012) 031909.
[33] H. Tanaka, S. Neukermans, E. Janssens, R.E. Silverans, P. Lievens, J. Chem. Phys. 119 (2003) 7115.
[34] Z.J. Wu, Chem. Phys. Lett. 406 (2005) 24.
[35] N. Godbout, D.R. Salahub, J. Andzelm, E. Wimmer, Can. J. Chem. 70 (1992) 560.
[36] K. Wolinski, J.F. Hilton, P. Pulay, J. Am. Chem. Soc. 112 (1990) 8251.
[37] M.J. Frisch *et al.*, *Gaussian 09*, revision A.02, *Gaussian*, Inc., Wallingford, CT, 2009.
[38] P.K. Chattaraj, S. Segupta, J. Phys. Chem. 100 (1996) 16126.
[39] U. Hohm, J. Phys. Chem. A 104 (2000) 8418.
[40] R.G. Pearson, Acc. Chem. Res. 26 (1993) 250.
[41] G. Maroulis, D. Begué, C. Pouchan, J. Chem. Phys. 119 (2003) 794.
[42] I.K. Dmitrieva, G.I. Plindov, Phys. Scr. 27 (1983) 402.